特集：高輝度X線(Ⅱ)—MR放射光利用—

§2. 加 速 器

2-4-4. A Study on Impedance in TRISTAN MR

Chuang ZHANG

*National Laboratory for High Energy Physics**

The TRISTAN was operated as a light source at 8 GeV and 10 GeV during the later part of 1995. The lattice was modified, some new components were installed and more than half of normal cavities and all the superconducting RF cavities were removed from the ring to reduce the higher-order mode impedance. Under this new configuration, the impedance is measured though betatron tune, synchro-phase, bunch length and closed orbit vs. bunch currents. The results are discussed and compared to their calculated and previously measured values.

1. Introduction

After the completion of the high energy physics program, TRISTAN Main Ring (MR) was operated as a light source at 8 GeV and 10 GeV from middle of September to end of December, 1995. The lattice was modified so that a 5.4 m long undulator was able to be installed and a low-emittance beam could be achieved[1]. The performance of the TRISTAN MR light source was reported elsewhere in this issue of journal[2]. **Table 1** lists the major changes took place in the TRISTAN-MR light source (MR-LS) in comparison with it used to be as a collider ring (MR-CR).

It is one of our major interests, from the machine physics point of view and B-factory study, to understand the impedance behavior in the new configuration of TRISTAN MR. We calculated the impedance of four components in MR with ABCI[3] and compared the results with the measurement. The impedance (or loss factors) was measured with betatron tune, synchro-phase, bunch length by means of either streak camera (SC) or beam spectrum monitor (BSM), and closed orbit distortion (COD) as functions of bunch currents. The results are discussed and compared to their calculated and previously measured values.

2. Impedance calculated with ABCI

Four types of components were taken into consideration in our impedance calculation, namely

Table 1. A comparison between MR-LS and MR-CR

Configuration	*MR-LS*	*MR-CR*
Beam energy (GeV)	8–10	30
Particle species	e^-	e^+ and e^-
Number of APS cavities	40	104
Number of SC cavities	0	32
Number of GV bellows	32	104
Number of SD bellows	560	560
Phase advance per cell μ_x/μ_y	90°/90°	60°/60°
Bunch length σ_z (mm)	~5	~8
Sextupole arrangement	NISS	ISS

* National Laboratory for High Energy Physics 1-1 Oho, Tsukuba-shi, Ibaraki-ken, 305 Japan
On leave of absence from Institute of High Energy Physics, Beijing, China.
19 Yuquan Rood Beijing, 100039 P. R. CHINA
TELEFAX 86-10-6821-3374 e-mail zhangc@bepc 3.ihep.ac.cn

the RF cavities, the RF bellows, the gate valve (GV) bellows and shielded (SD) bellows. **Table 2** and **Table 3** give the computed transverse and longitudinal loss factors respectively. The calculation done with ABCI is 2-dimensional. For those components as shielded and gate valve bellows, whose cross section is not x-y symmetrical, we took a symmetric approximation with the vertical dimension and scaled to the x plane.

It can be found from the tables that RF cavities and their bellows provide a major part of loss factors on both transverse and longitudinal planes. With their large number, the shielded bellows play an important role in transverse loss factor, while they are still not important on the longitudinal plane. On the other hand, the transverse loss factor does not change much with bunch length, while the longitudinal loss factor significantly depends on the bunch length.

3. Impedance measured with tunes vs. bunch currents

When a particle beam displaces from its central orbit, it generates wake field in the environment and loss energy transversely. This wake may act back to the beam and cause tune shift. To measure this current dependent tune shift, the effective transverse impedance ($Z_{T,\,eff}$) and loss factor (k_T) can be obtained:

$$Z_{T,\,eff}=\frac{4\sqrt{\pi}\,E/e\sigma_z}{R\beta}\frac{d\nu}{dI_b} \tag{1}$$

$$k_T=\frac{4\pi f_0 E/e}{\beta}\frac{d\nu}{dI_b} \tag{2}$$

where E is beam energy, e is electron charge, f_0 is the revolution frequency, R is average machine radius, σ_z is bunch length, β is envelope function and ν is the betatron tune to be measured for different bunch currents I_b.

Tune shift as function of bunch currents was measured few times in TRISTAN MR-LS, the typical plots of $\nu_{x,y}$ vs. I_b are given in Fig. 1.

It was in our surprising that the measured $-d\nu_y/dI_b$ around 10 A^{-1} in MR-LS is even larger than what was measured for MR-CR in 1990 before RF cavities and other impedance components were removed from the ring ($d\nu_y/dI_b=-7.25\ A^{-1}$), while the $-d\nu_x/dI_b$ around 3 A^{-1} in MR-LS is smaller than it was in MR-CR (measured at the injection energy of also 8 GeV) of 5.7 A^{-1} [4].

The transverse impedance and loss factors calculated with eq. (1) and (2) using the measured average $d\nu/dI_b$ are given in **Table 4**.

It can be seen from the table that the measured values of horizontal loss factor are close to their calculated values, while on the vertical plane the measured values are about factor of 2 larger than they were calculated. The measurement suggests that some elliptical shaped components were missed in our impedance computation.

Table 2. Transverse loss factor calculated with ABCI (Unit: 10^{15} V/C/m)

σ_z (mm)	2.5	5.0	7.5	10.0	12.5	15.0
RF cavities 40	0.96	1.24	1.40	1.51	1.58	1.62
RF bellows 160	0.51	0.64	0.67	0.63	0.55	0.46
GV bellows 32	0.22	0.26	0.25	0.22	0.18	0.14
SD bellows 560	1.47	0.75	0.53	0.41	0.33	0.28
Total x	1.88	2.13	2.27	2.29	2.25	2.19
y	3.15	2.88	2.86	2.76	2.63	2.50

Table 3. Longitudinal loss factor calculated with ABCI (Unit: 10^{14} V/C)

σ_z (mm)	2.5	5.0	7.5	10.0	12.5	15.0
RF cavities 40	3.90	2.94	2.46	2.14	1.90	1.71
RF bellows 160	1.51	0.91	0.58	0.34	0.19	0.10
GV bellows 32	0.22	0.12	0.07	0.04	0.02	0.01
SD bellows 560	0.54	0.10	0.04	0.02	0.01	0.01
Total	6.17	4.07	3.15	2.54	2.12	1.83

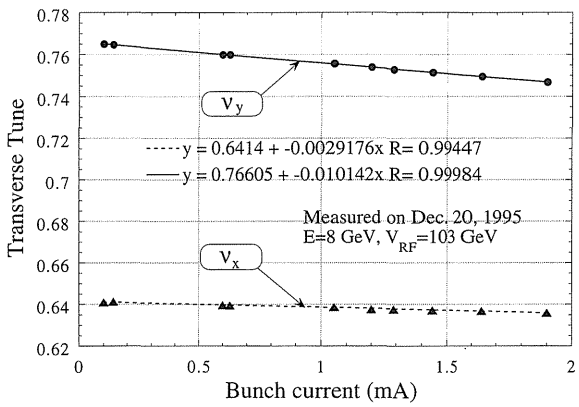

Figure 1. Horizontal and vertical tunes as functions of bunch currents.

Table 4. Impedance and loss factor obtained from measurement

V_{RF}	103 MV		50 MV	
bunch length (mm)	~5.0		~7.5	
direction	x	y	x	y
$d\nu/dI_b$ (A^{-1})	−3.283	−9.982	−2.836	−9.522
$Z_{T,eff}$ (kΩ/m)	160	337	208	482
k_T (10^{15} V/C/m)	2.71	5.70	2.34	5.44
$k_{T,mes}/k_{T,cal}$	1.27	1.98	1.03	1.90

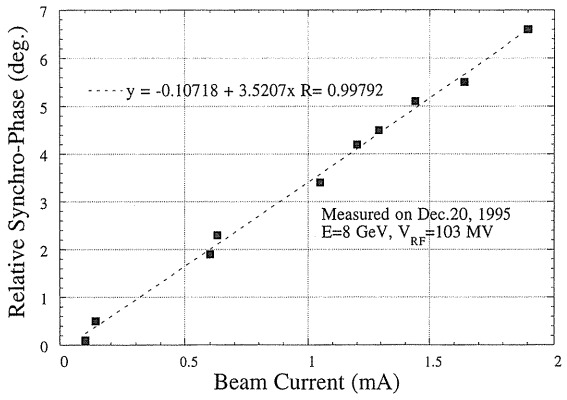

Figure 2. Synchro-phase for different beam currents.

4. Impedance measured with Synchro-phase vs. beam currents

Beam energy loss for various reasons in synchrotrons is compensated by RF cavities owing to the phase stability. The major part of the energy loss in electron machines comes from synchrotron radiation:

$$U_0=\frac{C_\gamma}{2\pi}E^4\int_{\text{dipoles}}\frac{ds}{\rho^2} \tag{3}$$

where U_0 is the energy loss per turn, ρ is the bending radius and C_γ is radiation constant. In practical units of MeV for U_0, GeV for E and m for ρ, $C_\gamma=0.0885\ \text{m}\cdot\text{MeV}/\text{GeV}^4$. In TRISTAN MR-LS at 8 GeV, $U_0=3.93$ MeV when the dumping wigglers were powered.

The synchro-phase change due to synchrotron radiation does not depend on beam intensity, but it does for the parasitic energy loss. The energy loss in accelerator rings due to impedance is proportional to the longitudinal loss factor as an integral over the real or resistive part of longitudinal impedance times the bunch spectrum. This provides a way to determine the longitudinal loss factor by means of measuring the synchro-phase (or RF phase) ϕ_s change in respect to beam currents:

$$k_L=f_0V_{RF}\cos\phi_s\frac{d\phi_s}{dI_b} \tag{4}$$

The synchro-phase as function of beam current was measured, shown in **Fig. 2**.

The linear fit for the ϕ_s vs. I_b curve in **Fig. 2** gives $d\phi_s/dI_b=3.52°\text{mA}^{-1}=61.5\ \text{rad/A}$, and yields $k_L=6.29\times10^{14}\ \text{V/C}$ for the bunch length roughly 5 mm, which is about factor of 1.5 larger than it was calculated. Again, this assumes that some of the impedance sources have not yet been taken into computation.

5. Bunch length measurement

Bunch lengthening (shortening) is one of the most interesting and confusing issues in synchrotrons. There are two processes in the bunch lengthening, i.e. potential well distortion and microwave instability (or turbulent bunch lengthening). A phenomenological model[5] provides a relation for potential well bunch length

$$\left(\frac{\sigma_z}{\sigma_{z0}}\right)^3-\frac{\sigma_z}{\sigma_{z0}}+\frac{\alpha_p e\left(\frac{R}{\sigma_{z0}}\right)^3}{\sqrt{2\pi}E\nu_s^2}\left(\frac{\text{Im}Z_L}{n}\right)_{\text{eff}}I_b=0 \tag{5}$$

where α_p is momentum compaction factor, ν_s is the synchrotron tune and $n=f/f_0$ is the mode number. In the case of inductive impedance ($\text{Im}(Z_L)<0$), the solution of the cubic equation eq. (5) gives $\sigma_z/\sigma_{z0}>1$, i.e. bunch lengthening is resulted. While in the capacitive impedance case ($\text{Im}(Z_L)>0$), bunch shortening takes place.

For the microwave instability, Boussard-Keil-Schnell formula[6] gives a 1/3 power dependence as

$$\sigma_z=\left(\frac{\alpha_pR^3}{2\pi E/e\nu_s^2}\right)^{1/3}\left|\frac{Z_L}{n}\right|I_b \tag{6}$$

The phenomena in the real machine are more complicated than they are described by the phenomenological model. A computer code was developed by K. Oide and K. Yokoya to simulate intensity dependence bunch length[7]. Taking advantage of the code, the current dependent behavior of bunch length was simulated by using the wake func-

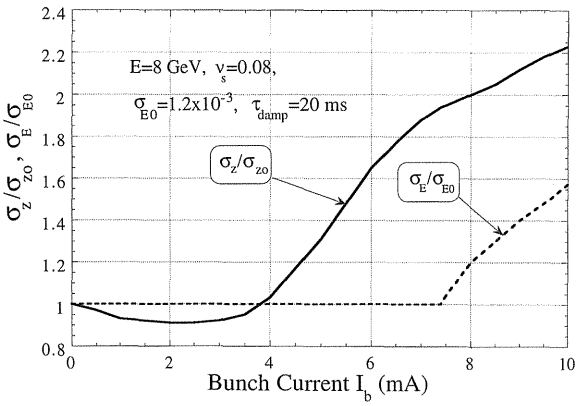

Figure 3. Simulated bunch lengthening (shortening) and widening.

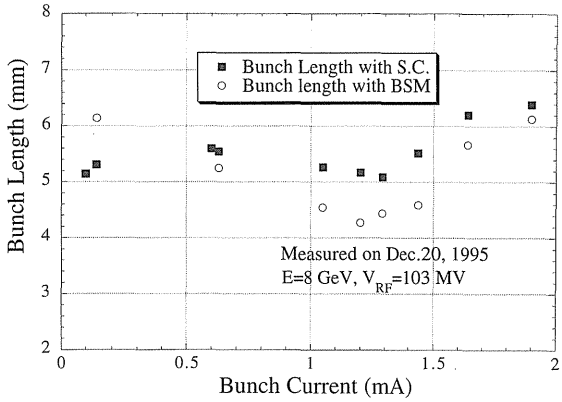

Figure 4. Measured bunch length as function of bunch currents.

tion computed with ABCI. The result is displayed in **Fig. 3**.

Two methods were applied to measure the bunch length in TRISTAN-MR, i.e. streak camera and bunch spectrum monitor. Steak camera provides an absolute bunch length, while the spectrum monitor gives a relative values. Knowing the bunch length at low current as nature bunch length, the BSM can be calibrated and used to measure bunch length at higher currents, assuming the distribution remains Gaussian. By careful calibration for BSM, its measurement accuracy could be better than 1 mm. A detailed description on the bunch length measurement in TRISTAN can be found in the reference[8]. **Fig. 4** displays bunch length as function of bunch currents measured with both SC and BSM.

It can be found from comparing **Fig. 4** with in **Fig. 3** that the measured bunch length curve is similar to but somehow different from the simulation. Both measurement and simulation show the bunch shortening at low currents. This is understood as the effect of reach capacitive impedance components in the RF cavities. But the bunch started lengthening around 1.5 mA in the measured curves, while it is about 4 mA in the simulation. This could be explained as the calculation does not provide enough inductive impedance into the simulation.

6. Local Longitudinal Loss Factor

Electrons lose their energy in the ring due to synchrotron radiation, interaction with metal environment and other mechanisms, while gain energy from the RF cavities so that the tip of the energy saw is right at the exit of the cavities and the base at its entrance. The energy saw can be measured with beam position monitors (BPM) in the regions with non-zero dispersion. However, in order to measure the parasitic energy loss due to beam-environment interaction in the ring, the contribution of the synchrotron radiation should be taken out.

The parasitic energy loss in the RF regions is compensated simultaneously by the cavities themselves. By using BPM's, one may measure the local property of the longitudinal loss factor in other parts of the ring as

$$k_L=\frac{Ef_0}{e\eta_x}\frac{\Delta x_{c.o.}}{\Delta I_b} \tag{7}$$

where η_x is the dispersion at the local component and $\Delta x_{c.o.}$ is the orbit change for the differential bunch currents ΔI_b. It is found from **Table 3** that k_L contributed by gate valve bellows and shielded bellows is about 2×10^{13} V/C for $\sigma_z=5$ mm, which may cause an energy loss $dE/dI_b=ek_L/f_0=0.2$ MeV/mA or an orbit displacement of 0.01 mm/mA at the maximum dispersion of 0.5 m in the MR light source configuration. This shows that it is possible but difficult to detect the local longitudinal loss factor in TRISTAN MR where the BPM resolution is around 20~50 μm[9].

6.1 Orbit scaled with bunch currents

The distribution of the energy loss around the ring can be obtained by comparing the orbit difference for two bunch currents. The measurement was done for different bunch currents from 0.1 mA to 2.0 mA at RF voltages of 103 MV, 50 MV and 20 MV. The bunch length measurement in

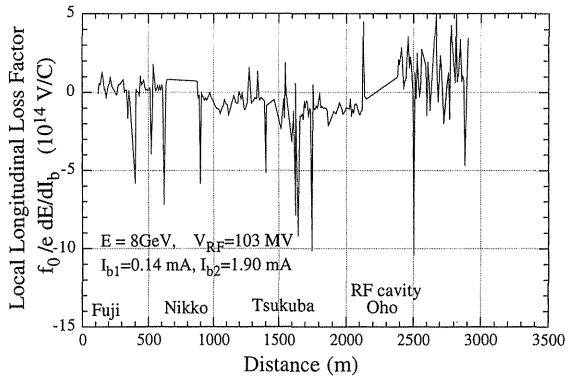

Figure 5. Measured longitudinal loss factor.

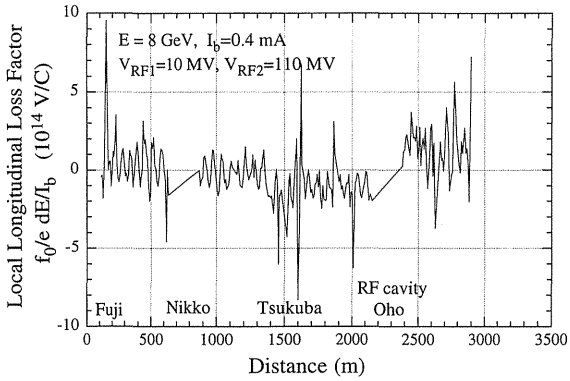

Figure 6. Measured differential longitudinal loss factor.

TRISTAN MR, described in the last section, shows no significant lengthening or shortening in this bunch current range. **Fig. 5** displays the distribution of longitudinal loss factor measured with BPM's. The step between exit and entrance of the RF cavities in Oho region shows the total loss factor in the ring other than the cavities.

6.2 Orbit scaled with RF Voltage

It can be found from **Table 3** that the longitudinal loss factor reduces significantly with increasing bunch length. This provides a way to investigate the differential loss factor around the ring for the different RF voltages. The orbit was measured for a bunch current of 0.4 mA with RF voltages of 10, 15, 30, 50, 70, 90 and 110 MV. Each of the orbit sets is compared with the orbit at 10 MV when the bunch length is the longest of about 15 mm. The differential loss factor is expressed as

$$\Delta k_L = \frac{Ef_0}{e\eta_x}\frac{\Delta x_{c.o.}}{I_b} \tag{8}$$

Fig. 6 displays the differential loss factor for V_{rf1} = 10 MV and V_{rf2} = 110 MV.

6.3 Discussion

The energy saw due to the parasitic energy loss can be seen in **Fig. 5** and **Fig. 6**, which show that the method of measuring the longitudinal loss factor by using BPM's is feasible. However, for such a small orbit change, the error of BPM reading of a few tens micro meter adds the evident ripple on the measured curve of loss factor. The measured longitudinal loss factor in the ring for different bunch lengths is plotted in **Fig. 7** together with the calculated loss factor of gate valve bellows and shielded

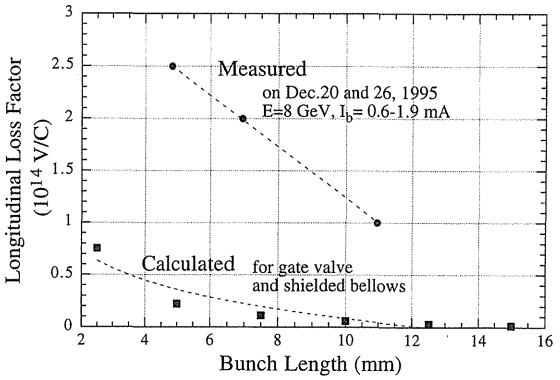

Figure 7. Measured and computed k_L vs. I_b.

bellows, which indicates that the measured k_L is obviously larger than the calculated values. Their difference at σ_z=5 mm is about the value of $k_{L,mes} - k_{L,cal} = 2.2 \times 10^{14}$ V/C. Similar results can be found in the differential loss factor measurement, shown in **Fig. 8**. The measurement suggests that there are other non-negligible impedance sources, such as resistive-wall, masks, BPMs, pumping slots and etc., in the TRISTAN MR while the measured loss factor distribution may help to locate the hidden sources.

The method of longitudinal loss factor measurement by using BPM's is demonstrated in TRISTAN MR-LS. Due to the small energy loss in the ring and the low dispersion function in the light source configuration, the accuracy of BPM is of prime importance for this measurement. In the KEKB case, the accuracy of BPM is improved by a factor of 5, while the expected longitudinal loss factor is one order lower than of TRISTAN MR. However, with the factor of 2 larger dispersion, the local loss factor could also be detected using this

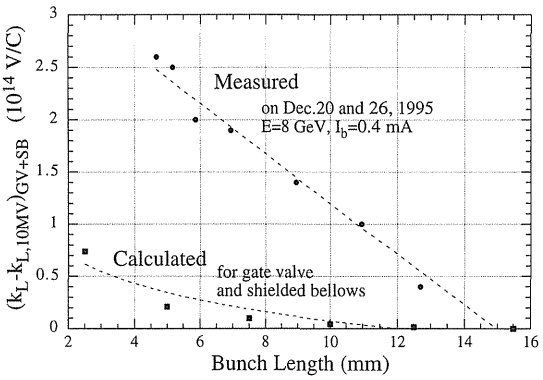

Figure 8. Measured and computed Δk_L vs. I_b.

method.

7. Summary

Four methods, i.e. tune vs. bunch currents, synchro-phase vs. beam currents, energy saw measurement and bunch length vs. currents, were applied to investigate the impedance and loss factors in TRISTAN MR-LS. The results with first three methods are summarized in **Table 5** together with the data for MR-CR measured in 1990.

It can be seen from **Table 5** that the measurement had been in a good agreement with the calculation for MR-CR carried out in 1990, but it was not the case for MR-LS done in 1995. How to explain the contradiction? The major changes took place in TRISTAN MR-LS are listed in **Table 1**. The purpose of removing RF cavities is to reduce the impedance, and it is hard to say how do other changes listed in **Table 1** influence on the impedance. However, the installation of the undulator and the beam line may introduce some discontinuities in the machine.

On the other hand, the measured loss factors for MR-LS are significantly larger than they were calculated. The tune vs. bunch current measurement

Table 6. Computed loss factors with ABCI and URMEL (σ_z=10 mm)

	Transverse (V/pC/m)		Longitudinal (V/pC)	
	ABCI	URMEL	ABCI	URMEL
3-cell APS cavity	12.6	12.6	1.78	1.78
RF bellows	3.92	3.86	0.213	0.208
GV bellows	6.82	6.50	0.117	0.108
SD bellows	0.737	0.664	0.0040	0.0037

Table 5. A comparison of calculated and measured loss factors

		MR-LS			MR-CR
V_{RF} (MV)		103	50	20	91
σ_z (mm)		~5	~7.5	~12	~8
Tune vs. bunch current measurement					
$k_{x,cal}$	(10^{15} V/C/m)	2.13	2.27	2.26	4.56
$d\nu_x/dI_b$	(A^{-1})	−3.283	−2.836	−2.13(?)	5.70
$k_{x,mes}$	(10^{15} V/C/m)	2.71	2.34		4.54
$k_{x,mes}/k_{x,cal}$		1.27	1.03		0.99
$k_{y,cal}$	(10^{15} V/C/m)	2.88	2.86	2.64	5.78
$d\nu_y/dI_b$	(A^{-1})	−9.982	−9.522	−6.33(?)	7.25
$k_{y,mes}$	(10^{15} V/C/m)	5.70	5.44		5.77
$k_{y,mes}/k_{y,cal}$		1.98	1.90		0.99
Synchro-phase vs. beam currents measurement					
$k_{L,cal}$	(10^{14} V/C)	4.07	3.15	2.20	7.54
$d\phi_s/dI_b$	(rad/A)	61.5			67.0
$k_{L,mes}$	(10^{14} V/C)	6.29			6.9
$k_{L,mes}/k_{L,cal}$		1.55			0.91
Energy saw measurement					
$k_{L,cal}^{(GV+SB)}$	(10^{14} V/C)	0.22	0.11	0.038	
$k_{L,mes}^{(arc)}$	(10^{14} V/C)	2.5	2.0	1.0	
$k_{L,mes}^{(arc)}-k_{L,mes}^{(GV+SB)}$		2.3	1.9	1.0	

gives the vertical loss factor of factor of two larger than calculated; the synchro-phase measurement shows 50% larger than calculation, while the measured energy saw indicates the longitudinal loss factor in the arc is much lager than calculated for GV and SD bellows. Here arises a question that if the measurement is reliable? The answer should be positive according to the discussion in the previous sections. Or conversely, if the calculation is reliable? The loss factors computed with ABCI are compared with those with URMEL[10] in **Table 6**. The table tells that they agree each other well. However, both of them are two-dimensional codes and the results for those non-symmetric components like shielded bellows and gate valve bellows need to be checked with a three-dimensional code.

The comparison between the measurement and the calculation suggests that there are some impedance components out of our scope of computing, such as resistive-wall, kickers, separators, masks, BPM's, beam lines, pumping slots and others and other discontinuity, which need to be investigated further.

Acknowledgment

The investigation on the impedance in TRISTAN MR and relevant machine studies are team work of whole TRISTAN Light-Source Commissioning Group. The author wish to thank S. Kamada, H. Fukuma, Y. H. Chin, Y. Funakoshi, K. Ebihara, S. Matsumoto, A. Ogata, T. Ieiri, M. Tobiyama and other group members for the friendly collaboration and helpful discussions.

References

1) S. Kamada et al.: Rev. Sci. Instrum., Feb. (1995).
2) H. Fukuma : issue of the journal.
3) Y. H. Chen: CERN SL/94-02, (1994).
4) K. Satoh: Private communication, (1995).
5) A. W. Chao: Wiley-Interscience Publication, (1993).
6) D. Boussard: CERN Lab. II/RF/Int./75-2, (1975).
7) K. Oide and K. Yokoya: KEK preprint 90-10, April (1990).
8) T. Ieiri, M. Tobiyama and C. Zhang: Workshop on TRISTAN MR-LS, Jan. (1996).
9) H. Ishii et al.: Proc. 6-th Symp. Acc. Sci. and Tech., (1987).
10) T. Weiland: DESY M-82-24, (1983).